Runway Centerline Deviation Estimation from Point Clouds using LiDAR Imagery

Zoltan Koppanyi
SPIN Lab
The Ohio State University
Columbus, OH, USA
koppanyi.1@osu.edu

Charles K. Toth
SPIN Lab
The Ohio State University
Columbus, OH, USA
toth.2@osu.edu

Seth Young
Center for Aviation Studies
The Ohio State University
Columbus, OH, USA
young.1460@osu.edu

***Abstract*—Secure airport operations are an important part of the aviation safety, as about 20 percent of collisions between aircrafts and objects as well as about one third of fatal accidents occur on airfields. The older airports need to be modernized to better cope with increasing traffic and larger aircrafts. Determining proper separation distances or safety areas is part of the revision process. In addition, engineering, environmental and economic impacts have to be considered during such revisions. To support the redesign, statistically significant and representative data is needed, including driving patterns and various derived metrics, such as centerline deviations. Remote sensing technologies offer an effective way to collect large volume of data on aircraft movements at airfields. This study describes the initial results of a LiDAR-based multi-sensor system that is deployed around runways and taxiways to remotely observe aircraft movement. The primary objective is to derive the centerline deviation of moving aircrafts from point clouds. Benefits from these derivations may allow for greater understanding of aircraft movements in the runway environment, and provide data for evaluating the operational safety of various runway design specifications.**

Keywords-component; laserscanning; feature extraction; mostion estimation; aircaft centerline deviation

I. INTRODUCTION AND BACKGROUND

This paper presents the results of research designed to develop a low cost yet effective remote sensing technology for the purpose of tracking aircraft movements along a runway during takeoff and landing, specifically, to address a need to further understand how "accurately" general aviation aircraft track along the centerline of a runway during such operations. This need was presented to the authors by the Federal Aviation Administration (FAA) who desired to study the deviations from runway centerline for such aircraft during takeoff and landing operations.

The FAA's desire for this understanding has been motivated by the fact that increasingly larger and higher performance aircraft are utilizing general aviation runways originally designed for slower and smaller aircraft. As a result, there may be some concern that such aircraft may be more prone to runway excursions, defined as the unintended overrun or veer-off from the runway during a takeoff or landing. Conversely, should aircraft be found to be using runways with high degrees of accuracy, i.e., minimal deviation from centerline, the FAA may be able to justify alterations in minimum runway and associated safety area specifications [1].

Remote sensing technologies may offer a simple, yet reliable way to acquire centerline deviation of aircraft operations on airport runways. Sensors can be deployed around runways and precise information can be obtained without any assistance from the aircraft. Previous studies have proven the feasibility of such technologies for aircraft movements on taxiways. To study taxiing behavior, [2] used positioning gauges to obtain data at the Chiang-Kai-Shek International Airport, Taiwan. The gauges recorded the passing aircraft's nose gear on the taxiway. Another study by FAA/Boeing investigated the 747s' taxiway centerline deviations at JFK and ANC airports [3, 4]. They used laser diodes at two locations to measure the location of the nose and main gears. Another report deals with wingspan collision using the same sensors [5]. The sensors applied and investigated by these studies allow only point type data acquisition; detecting the light bar passing.

Imaging sensors are especially effective to acquire large volume of data to extract objects, such as aircraft bodies, and then track them based on image sequences. Most of these imaging sensors, such as the W-Band radar sensing technology used by Synthetic Air Traffic Advisory System (SATAS) [6] or camera surveillance systems, are applicable for tracking the aircraft on or close to the ground, but their accuracy does not achieve the level which is required for the precise centerline deviation estimation.

This paper reports about some aspects of the authors' ongoing research at investigating the feasibility of LiDAR (Light Detection and Ranging) technology to estimate the

Support from the PEGASAS FAA program is greatly appreciated.

centerline deviation of taxiing/landing aircraft. LiDAR is an active imaging spatial data acquisition method that enables to directly capture 3D points from the environment [7, 8]. The contribution of this study is to describe a new method for extracting centerline deviations, as the distance between the centerline and the aircraft's front gear, from point clouds provided by multiple LiDAR sensors. The description includes the experimental sensor system, the data acquisition component and the data processing methods to estimate the aircraft movement with respect to the centerline, and the probability curves of the centerline deviation and veer-off location.

II. METHOD

A. Sensor network

In this investigation, Velodyne VLP-16 sensors are used due to their relatively high, 10 Hz, sampling rate and moderately low cost [9]. This sensor is able to make a 360° scan with 0.6° angular resolution around the rotation axis and contains 16 laser diodes perpendicularly installed to the rotation plane enabling for 30° field of view (FOV) along this direction with a 2° sensor separation. The Velodyne VLP-16 scanning rate of 10 Hz results in 0.1°-0.4° with affective 0.2° average separation between consecutive shots of a single laser diode, equaling in a linear separation around 10 centimeters at the scanning distance of 30 meters. For data acquisition, a sensor network is established with four VPL-16 sensors; two scanners are attached to a standard airfield light fixture's metal column, see Fig. 1.

One light fixture is equipped with two vertically orientated scanners (i.e. the scanner's rotation plane is perpendicular to the runway, left side of Fig. 1) and the other installation has one horizontally and one vertically oriented scanners (right side of Fig. 1). Regarding the sensor orientations, as the installation shows, the horizontal orientation was preferred, because the investigation by [10] using a Velodyne HDL-32E sensor and by [11] based on simulated data, proved the benefits of horizontally orientated profile scanners. Clearly, this orientation allows to acquire larger number of points across the aircraft body than the vertically oriented sensor. The limitation of horizontal rotation is the small horizontal FOV, and, consequently, only a small section of the runway/taxiway can be monitored.

Since the time information is critical for any data integration and sensor fusion, such as tracking the aircraft motion from point clouds acquired by multiple sensors, the scanners receive navigation messages (NMEA) and the 1PPS (Pulse Per Second) signal for precise timing sent by a GPS receiver via the scanner interface box to GPS time tag the recorded data. This solution provides a very accurate time synchronization among the laser sensors.

The experimental sensor network was installed adjacent to Runway 9L, a 1000 meter long, 30 meter wide, general aviation runway at The Ohio State University Airport (Airport). The sensor arrangement with the FOV for each scanner is shown in top view in Fig. 2. The two sensor assemblies were placed ~25 meters away from the centerline.

Figure 1. Velodyne sensors attached to the light fixture post

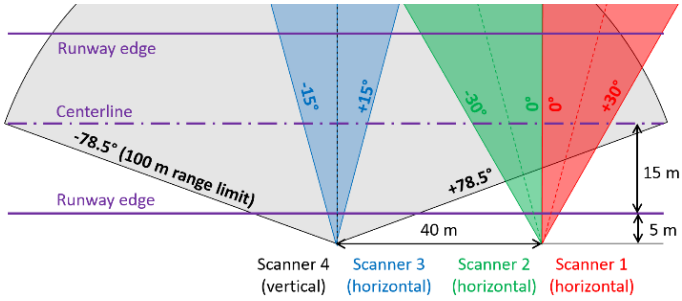

Figure 2. Four scanner configuration (drawing not to scale)

On the right side of the figure, the two vertical-aligned sensors (Scanner 1 and 2) cover 60° of the runway, while on the left side, Scanner 3, perpendicular to the centerline, and the horizontally orientated Scanner 4 capture the data. The distance between the two sensor locations is 40 meters, and thus the effective coverage of the system is 50 meters, because those points that are outside of the three vertical scanners FOV, and captured only by Scanner 4 cannot be used in the calculations due to the sparsity at longer ranges. This coverage allows approximately 3.5 seconds data acquisition depending on the aircraft velocity. In the future, the plan is to extend the sensor network with further equipment, such as using Velodyne HDL-32E sensor for horizontal scans. Note that this sensor is more expensive, but the perpendicular FOV is wider and the angular resolution is also smaller due to the 32 laser diodes, and consequently, more points can be observed horizontally.

B. Data processing

The sensors capture the X, Y, Z coordinates of the points in the sensor coordinate system and each point is tagged with GPS synchronized timestamp provided in UTC. To transform all points to a local frame or an absolute mapping frame, the orientation and position need to be for each scanner in the same frame. An important aspect of a multisensory system is the spatial relationship of the various sensors, including the location and orientation of all sensors in the local frame. The orientation of point clouds was performed in two steps. First, scans are

aligned to the surface of the runway and then rotated according to known azimuth. For the simplicity, in many cases, it can be assumed that the surface of the runway is planar and horizontal, otherwise, additional measurements are necessary to estimate the normal vector of the runway observed by each scanner. Then the normal vectors are estimated based on the non-transformed point clouds in the areas corresponding to the runway area. Based on a pair of corresponding normal vectors, the point cloud can be rotated to match the runway surface, leaving only the azimuth unknown. This problem can be solved by finding and using straight objects in the point cloud. For example, the rotation angle/azimuth can be found by estimating the direction of the runway pavement markings in the point cloud and measuring them in the field.

The transformed point cloud contains not just the point of the aircraft body, but other points from the environment. The next step of the data processing is to remove the non-aircraft points from the dataset and keep only the relevant part. Additionally, in case of a long-term data acquisition, it is also difficult to find the time frames when the aircrafts are in the sensors' FOV.

To overcome these problems, firstly, region of interest (ROI) has to be selected where the aircraft possibly moves. The ROI is a 3D box that covers the runway X-Y plane with a Z limit that is the expected height of the airplanes. In the second step, the point cloud changes have to be tracked inside the ROI. The point cloud changes are detected separately for each sensor by calculating the amount of the points captured by a full 360 degree scan. This full scan is called a frame. The blue line in Fig. 3 shows the cloud sizes within the frames captured by the horizontally aligned Sensor 4. The peaks show the possible places when a plane might have crossed the sensor FOV. Based on Fig. 3, a threshold can be easily selected where a detection is likely.

But, as Fig. 3 shows, the end of the data, after frame 9500, is lower compared to the beginning. Note that this dataset was observed by Sensor 4, aligned horizontally, and thus, it is able to capture only three or four stripes from the aircraft body due to the 2° separation along the vertical direction. Therefore, if the plane-sensor relative position is not favorable, the detected point number may be low, causing discrepancies, and the plane detection based only on cloud size does not give a robust solution.

Another potential method is to decimate the place with a given size of cubes and then counting those cubes that are occupied by points. This way, the changes can be detected as the changes of the occupied cubes between the consecutive frames. To improve the robustness of this solution, one cube is marked as occupied if it contains at least 5 points. This allows to avoid the miss detections caused by backscatters from different small object flying in the air, etc. The red data series shows these cube changes in Fig. 3, illustrating that the cube-based approach provides similar differences at the beginning and at the end.

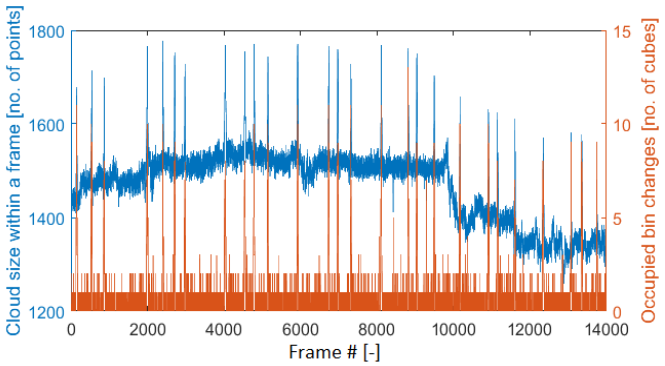

Figure 3. Point number and bin number changes between frames from Sensor 4

C. *Aircraft pose estimation*

1) *Challanges*

After filtering the points from the environment, the dataset is ready for the aircraft pose estimation. Fig. 4 shows an example of the point clouds at various times from a jet at about 30 meter object-sensor distance. Note that the point cloud is very small compared to other laser scanner applications. For example, it is obvious that just by calculating the gravity center of the points within the frames is not an applicable way to calculate the aircraft position. Furthermore, the trajectory estimation is a challenging problem due to the fact that the frames do not contain the entire aircraft body and, consequently, partial point sets have to be used for the estimation. However, this problem can be constrained by the motion with assuming a dynamic model, and thus, the problem space can be reduced.

2) *Motion model*

The aircraft body motion can be describe with a constant velocity (CV) model:

$$\begin{aligned} \Delta x &= v_x \Delta t \\ \Delta y &= v_y \Delta t \\ \Delta z &= v_z \Delta t \end{aligned} \tag{1}$$

where $\Delta x, \Delta y, \Delta z$ are the displacements of the aircraft body, Δt is the time from the reference, v_x, v_y, v_z are the x, y, z components of unknown constant velocity. If the velocities are known, and a motion model is assumed, all of the points captured at any epoch can be calculated back to the zero time resulting in a reconstructed point cloud of the aircraft body. Point cloud reconstruction is a method that enables to transform the points into a same coordinate frame. The shape or consistency of this reconstructed point cloud can be directly used for an initial visual assessment of the derived parameters.

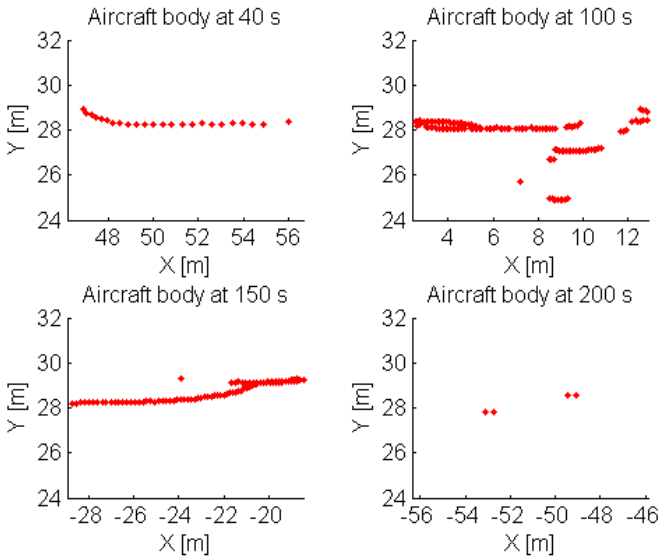

Figure 4. Backscattered points from the aircraft body at various times from the same sensor

3) Solution of the motion model

In our previous study, we have already introduced a method to estimate motion parameters [10]. This method is called the volume minimization (VM) algorithm. The idea behind this approach is that at the optimal parameters the reconstructed point cloud occupies the smallest space. Each realization of the parameters determines a reconstructed point cloud and after decimating the space into cubes, the algorithm tries to find those parameters in which case the bin numbers occupied by the reconstruction is minimal. Our previous studies indicated that the VM algorithm can be enough accurate to determine centerline deviations [10, 11].

4) Trajectory calculation

The CV model describes a uniform motion and, thus, has some limitations [12]. The aircraft body is assumed to follow a rigid body motion and the heading of the aircraft is always in the direction of the motion. As no acceleration is present, this nonmaneuver model is not able to describe curvy or any other motion that contains turns, and thus it can be only valid for short time periods. Thus, during the data processing, a CV model is solved by the VM algorithm with the point clouds found in the range of the moving time window, as it advances forward. The VM estimation always gives a solution within this new window.

After running through the dataset, the v_x^i, v_y^i, v_z^i velocities are known within the i^{th} time window, and t_p time is also calculated as the midpoint of the time window, see Fig 5. The position of the aircraft body at t_p can be calculated with the integration of the velocity curves. Since our "sampling" gives discrete values, the trapezoidal numerical integration form substitutes the continuous integration:

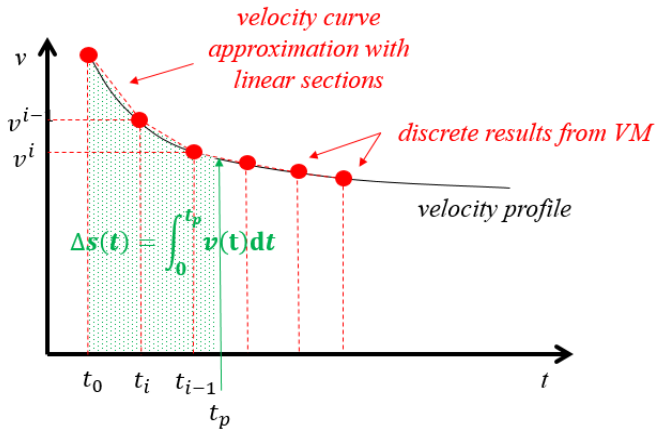

Figure 5. Approximation of the velocity curve with discrete samples obtained by constant model (CV)

$$\Delta x_p = \left[\sum_{\substack{j=2,\\ t_p<t_j}}^{n} \frac{v_x^i - v_x^{i-1}}{2}(t_j - t_{j-1})\right] + \frac{t_p - t_{j^*-1}}{t_{j^*} - t_{j^*-1}}\left(v_x^{j^*} - v_x^{j^*-1}\right) + v_x^{j^*-1},$$

$$\Delta y_p = \left[\sum_{\substack{j=2,\\ t_p<t_j}}^{n} \frac{v_y^i - v_y^{i-1}}{2}(t_j - t_{j-1})\right] + \frac{t_p - t_{j^*-1}}{t_{j^*} - t_{j^*-1}}\left(v_y^{j^*} - v_y^{j^*-1}\right) + v_y^{j^*-1}, \quad (2)$$

$$\Delta z_p = \left[\sum_{\substack{j=2,\\ t_p<t_j}}^{n} \frac{v_z^i - v_z^{i-1}}{2}(t_j - t_{j-1})\right] + \frac{t_p - t_{j^*-1}}{t_{j^*} - t_{j^*-1}}\left(v_z^{j^*} - v_z^{j^*-1}\right) + v_z^{j^*-1}.$$

where $\Delta x_p, \Delta y_p, \Delta z_p$ are the displacements of the p point at t_p and j^* is the last index before t_p, namely $t_{j^*} < t_p : t_{j^*} > t_k, \forall k \in [1..n]$ and assuming $t_p > t_0$ and $t_p < t_n$. Eq. 2 allows to calculate the trajectory of the aircraft as well as to reconstruct the aircraft body.

D. Centerline deviation estimation

The previously calculated trajectory describes the motion of all of the points of the aircraft body. Here, the centerline deviation is defined as the distance between the runway's centerline and the aircraft's front wheel. Thus, if the front gear is known in the first frame, its relative position can be calculated at later time epochs. The reconstructed point cloud is used to extract the front gear position. This cloud contains all the points from the tracking, thus it encapsulates all information and details that is available from the aircraft body; note that it is easier to find the front gear from the point cloud. Furthermore this point

cloud is referred to the first frame, thus once the gear position is known, its trajectory is also known.

First possible gear points are selected from the point cloud by slicing it with a plane close to the ground. Knowing the approximate height of the gear, this plane can be positioned, and leaving room above and below it, the possible gear point set can be determined. Fig. 6 shows an example of the algorithm. The red points represent the reconstructed point cloud, the blue points are the possible gear point sets. The k-mean clustering algorithm can distinguish the different clusters of the point set. The cluster centroids provided by the algorithm are the gears and the center of other point clusters. The cluster corresponds to the front gear is located at the leftmost or rightmost depending on the motion direction. The front gear position is this cluster's centroid.

III. DATA ACQUISITION

During the test performed at the Airport, the data was acquired from 18 single piston engine Cessna 150 and 172 model airplanes performing "touch and go" (i.e. landing, followed by an immediate takeoff) operations, see Fig 7. Two scanner sets described earlier were placed at the same distance from the runway, separated by 34.8 m, as shown in Fig 2. At the selected scanning rate of 10 Hz, the time required to observe the moving aircraft by each scanner was about 1-1.2 seconds and 7 seconds for scanners 1-3 and 4, respectively.

The point clouds from all scanners were co-registered in the local coordinate system defined. The local coordinate system orientation and acquired point clouds are shown in Fig 8. For the centerline deviation estimation, not the entire dataset was used, only data between the FOV of Scanner 1 and Scanner 3, leftmost and rightmost vertical scanners, as the captured point cloud size by Scanner 4 is too small for reliable estimation outside of the FOV of the other sensors. Thus, the coverage of the test system is ~40 meters and ~3.5 seconds.

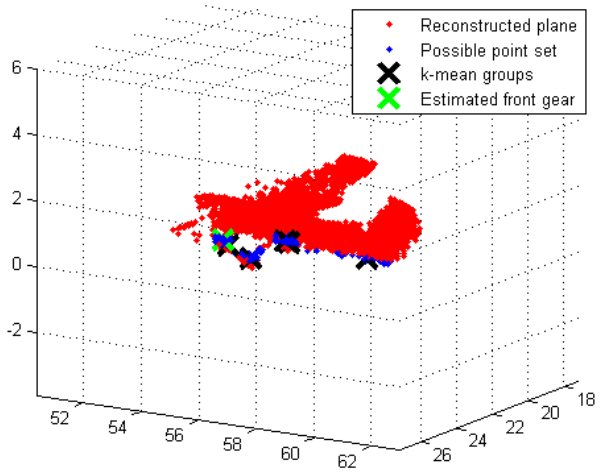

Figure 6. Estimated front gear.

Figure 7 Scanning of a landing airplane

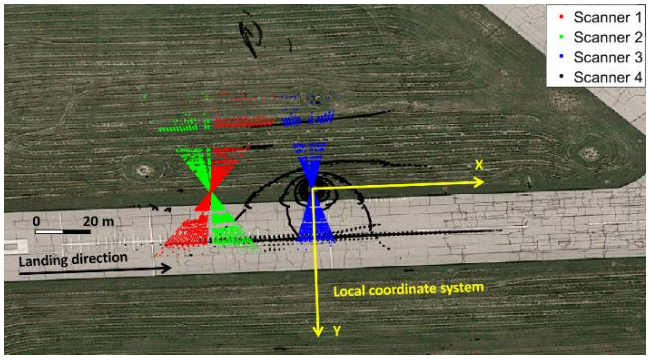

Figure 8. Acquired point clouds (top view)

IV. RESULTS AND DISCUSSION

After finding the aircraft in the dataset using ROI and detecting the occupied cube changes, the VM algorithm solves the CV model within the time frames. The 1 second time window goes through the data in 0.1 seconds steps. The trajectory is calculated with Eq. 2. Fig. 9 shows the reconstructed plane and the original point set. The visual inspection of the reconstructed plane can give some information about the accuracy of the method: the consistent and sharp edges mean good estimation. The black line in the Fig. 9 shows the estimated trajectory of the front gear that can be used for the centerline deviation calculation. Fig. 10 shows the velocity the velocity profiles. The X velocity shows a slight deceleration and also the Z component indicates a slight descent. As the sensor's rotation plane is perpendicular to the aircraft motion direction, the velocity along the Y direction provides information about the centerline deviation. Fig 11 shows the trajectory solutions (black) of the 18 tracked airplanes and the centerline with red dashed lines. Note that to better distinguish the different trajectories, the 1:5 exaggeration ratio is applied. The airplanes' movement patterns follow the centerline within ±1 meter.

The centerline deviation distribution can be estimated from the trajectory solution; Figure **12**Fig. 12 shows an example. Here, first, the histogram of the centerline deviation is calculated, and then a Gaussian distribution was fitted to the histogram points. This function can be estimated at different cross-sections; in our case, with five meter separation and they are depicted with colorized dashed lines in Fig. 11 and with same colors in Fig 12.

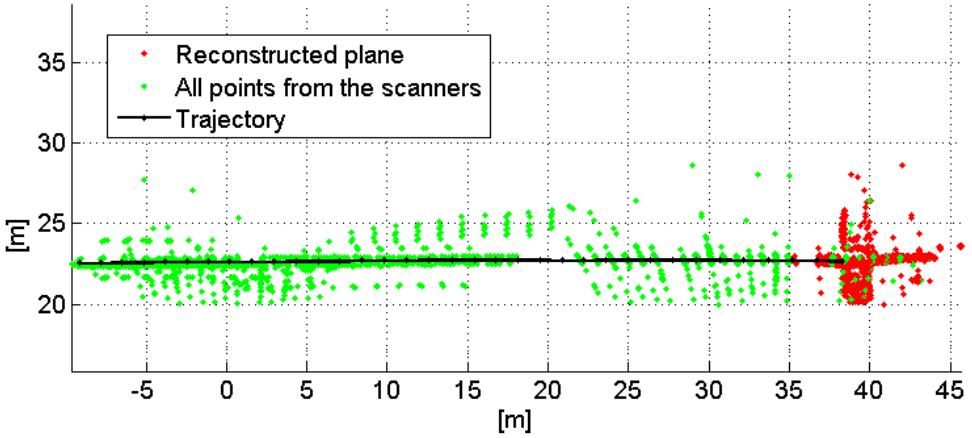

Figure 9. Reconstructed plane cloud, including all points from the sensors and the estimated trajectory

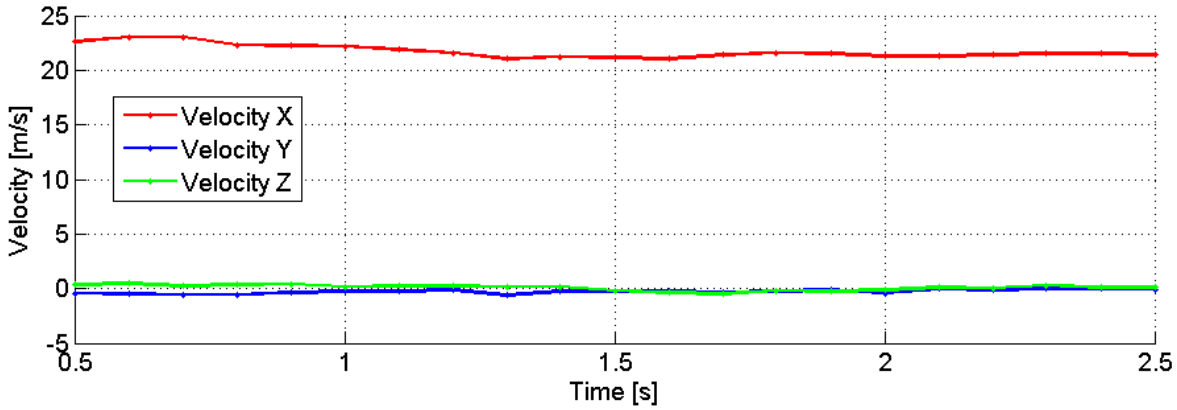

Figure 10. Velocity profiles along X, Y and Z directions

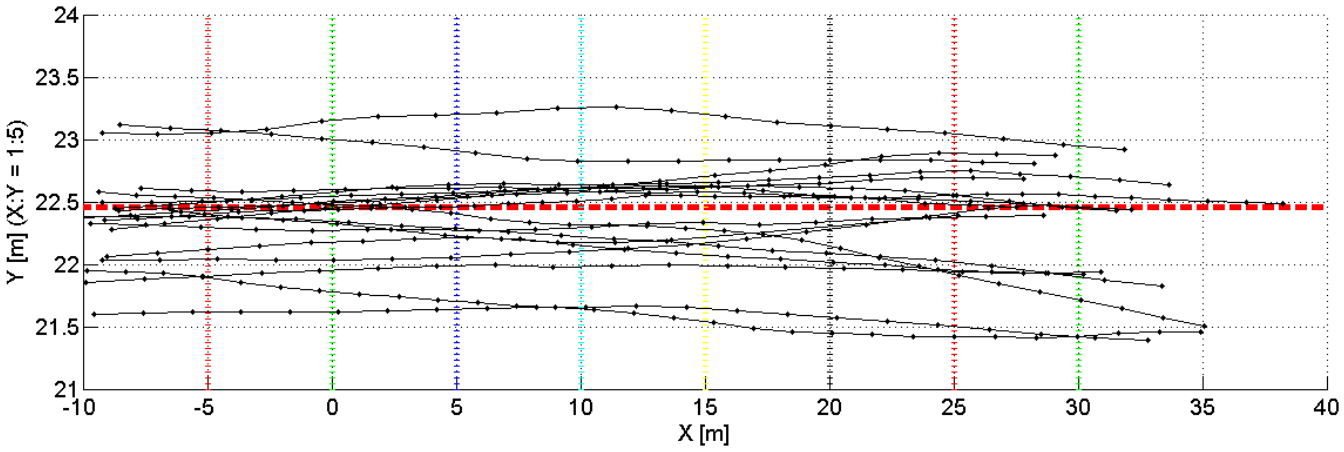

Figure 11. Estimated aircraft trajectories (black) and the centerline (red) (ratio: X:Y = 1:5)

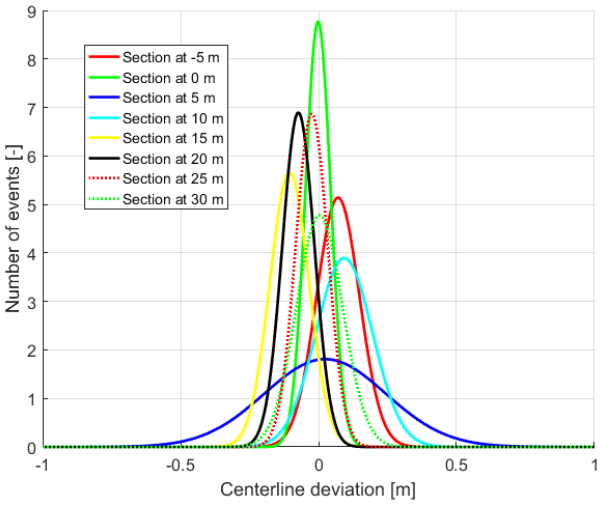

Figure 12 The Gaussian functions at various cross sections fitted to the centerline deviation histogram

The centerline deviations also allow developing location models, such as accident location model for runway excursion veer-offs. Following [13], this probability is modeled as an exponential function; higher probability corresponds to smaller deviation as the pilots try following the centerline. Smaller number of detection is expected to be observed with increasing the deviation. From the datasets, here, the following cumulative density function (CDF) is estimated:

$$F(y) = P(d > y) = -e^{-\frac{y}{\mu}}, \quad (3)$$

where d is the centerline deviation, and the μ parameter is determined with maximum likelihood estimation. This CDF can be estimated at different cross-sections, these sections are following each other with five meters separation and they are depicted with colorized dashed line in Fig. 11.

The exponential curves are shown in Figure 13. The circles with various colors show the points of the empirical cumulative distribution calculated from the absolute centerline deviations. The critical or dangerous range is at the tail. This interval is important to specify the thresholds or probabilities that may correspond to certain runway safety area dimensions, required runway-taxiway separations, or veer-off events. Of course, generally not enough observations are available in this range, because these events would imply dangerous situations, and thus it is rare to capture. Even if we would be able to capture one or two, the dataset is still not large enough to derive statistically relevant consequences. To derive information from this critical domain, extrapolation has to be applied. Another statistical approach can be the extreme value analysis [3, 4, 5], but this discussion is outside of the scope of this paper.

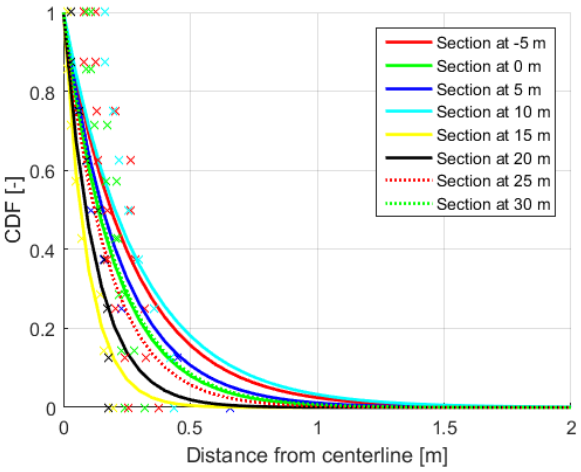

Figure 13. Relative histogram of the aircraft-centeline distances at different cross sections.

V. Conclusion and Future Work

This paper introduced a new data acquisition method based on LiDAR technology and data processing to derive centerline deviations. A concept of a sensor network are presented with the solution of the timing synchronization, network arrangement and installation.

Regarding the data processing, the first step is to remove those points that are out of the region of interest from the captured point clouds. Unfortunately, these captured point clouds contain small amount of points from the aircraft body. But, with assuming certain type of motion and estimating its parameters, the point clouds can be transformed into a common frame resulting in a reconstructed point cloud. Our previously proposed algorithm finds the optimal motion parameters by minimizing the volume of this reconstructed airplane. This method works well whether the motion is assumed to be uniform (i.e. constant velocity motion), but this kind of motion is only valid for short time periods. That's why, the trajectory is approximated with several constant velocity models and the final driving pattern, and thus, the centerline deviation can be derived as the numerical integration of the results of the constant models.

For validating our concept, a sensor network of four Velodyne's VPL-16 was deployed to an airfield and captured 18 airplanes. The point clouds of these airplanes are processed. From the derived point clouds the cumulative density functions at different sections of the runways were estimated. Since the CDFs are estimated from 18 airplane movement patterns, thus the presented curves is not applicable in the engineering design at this stage, but it proves that the presented methodology is usable and it is able to determine the center line deviations.

In the future, more airplanes are expected to be observed from a permanently installed system on a general aviation runway, and thus, a database can be created that will be used for

deviation analysis. Additionally, we also want to extend our network with other sensors, such as cameras and ultra-wide band units, to aid airplane detection and the driving pattern computation. An accuracy assessment of the calculated data are also required to understand the limitations. This validation can be solved using on-board GPS receivers as reference.

ACKNOWLEDGEMENTS

The authors would like to thank the Ohio State University Airport as the test site for this research and the Federal Aviation Administration who supported this work through the Center of Excellence for General Aviation, known as PEGASAS, the Partnership to Enhance General Aviation Safety Accessibility, and Sustainability. Although the FAA has sponsored this project, it neither endorses nor rejects the findings of this research. The presentations of this information is in the interest of invoking technical community comment on the results and the conclusions of this work.

REFERENCES

[1] ACRP Report 41: Risk Assessment Method to Support Modification of Airfield Separation Standards, URL: http://www.faa.gov/airports/resources/publications/reports/media/ANC_747.pdf (22 Apr 2016), p. 26

[2] C. Chou, H. Cheng., "Aircraft Taxiing Pattern in Chiang Kai-Shek International Airport" in Airfield and Highway Pavement Specialty Conference, April 30 – May 3, 2006, pp. 1030-1040, 2006

[3] F. Scholz, "Statistical Extreme Value Analysis of ANC Taxiway Centerline Deviation for 747 Aircraft (prepared under cooperative research and development agreement between FAA and Boeing Company)", The Boeing Company, *report*, Web link: http://www.faa.gov/airports/resources/publications/reports/media/ANC_747.pdf (22 Apr 2016).

[4] F. Scholz, "Statistical Extreme Value Analysis of JFK Taxiway Centerline Deviation for 747 Aircraft (prepared under cooperative research and development agreement between FAA and Boeing Company)", The Boeing Company, *report*, Web link: http://www.faa.gov/airports/resources/publications/reports/media/JFK_101703.pdf (18 Febr 2016).

[5] F. Scholz, "Statistical Extreme Value Concerning Risk of Wingtip to Wingtip or Fixed Object Collision for Taxiing Large Aircraft (prepared under cooperative research and development agreement between FAA and Boeing Company)", 2005, The Boeing Company, *report*, URL: http://www.airtech.tc.faa.gov/Design/Downloads/separation%20new.pdf (18 Febr 2016).

[6] URL: http://www.aopa.org/News-and-Video/All-News/2014/April/03/SATAS-demo (22 Apr 2016)

[7] J. Shan, C. K. Toth, Topographic Laser Ranging and Scanning: Principles and Processing, CRC Press, p. 616, 2008

[8] G. Vosselman, H.-G. Maas, Airborne and Terrastrial Laser Scanning, 1st edition, Whittles Publishing, p. 336, 2010

[9] URL: http://velodynelidar.com/vlp-16.html (22 Apr2016)

[10] Z. Koppanyi, C. K. Toth, "Estimating Aircraft Heading Based on Laserscanner Derived Point Clouds" in ISPRS Annals of Photogrammetry, Remote Sensing and Spatial Information Sciences, Vol. II-3/W41, pp. 95-102., 2015

[11] K. Dierenbach, G. Jozkow, Z. Koppanyi, C. K. Toth, "Supporting Feature Extraction Performance Validation by Simulated Point Cloud" in Proceedings of ASPRS 2015 Annual Conference, May 4 - 8, 2015, Tampa, Florida, USA.

[12] X. R. Li, V. P. Jilkov, "A Survey of Maneuvuring Target Tracking. Part I. Dynamic Models" in Aerospace and Electronic Systems, IEEE Transaction on., vol. 39, no. 4, pp. 1333-1364, 2003